Energy Transfer in Single-Molecule Photonic Wires

María F. García-Parajó,*[a] Jordi Hernando,[b] Gabriel Sanchez Mosteiro,[a] Jacob P. Hoogenboom,[a] Erik M. H. P. van Dijk,[a] and Niek. F. van Hulst[a]

Molecular photonics is a new emerging field of research around the premise that it is possible to develop optical devices using single molecules as building blocks. Truly technological impact in the field requires focussed efforts on designing functional molecular devices as well as having access to their photonic properties on an individual basis. In this Minireview we discuss our approach towards the design and single-molecule investigation of one-dimensional multimolecular arrays intended to work as molecular photonic wires. Three different schemes have been explored: a) perylene-based dimer and trimer arrays displaying coherent exciton delocalisation at room temperature; b) DNA-based unidirectional molecular wires containing up to five different chromophores and exhibiting weak excitonic interactions between neighbouring dyes; and c) one-dimensional multichromophoric polymers based on perylene polyisocyanides showing excimerlike emission. As a whole, our single-molecule data show the importance of well-defined close packing of chromophores for obtaining optimal excitonic behaviour at room temperature. Further improvement on (bio)chemical synthesis, together with the use of single-molecule techniques, should lead in the near future to efficient and reliable photonic wires with true device functionality.

The ultimate goal in device miniaturisation aims at the incorporation of single molecules as building blocks for the construction of molecule-based electronic, mechanical and optical devices. Molecular electronics, for instance, is emerging as a field that will conjecturally resolve the quest to scale electronics beyond the limit of "Moore's Law".[1] Yet, molecular devices will, for a broad range of applications, be driven or powered by light.[2] Decisive advantages of the photonic approach are flexibility of addressability (wavelength, polarisation), picosecond reaction times providing ultrafast speed for light transport or switching and the possibility of manipulating and/or tailoring output performance. Furthermore, quantum phenomena associated with light clearly manifest at room temperature, in contrast with the low-temperature requirements of molecular electronics.

Molecular photonics, as field of research at the strategic intersection of chemistry, physics and engineering sciences, is rapidly emerging as realistic alternative to eventually complement the rather mature semiconductor-based technology, which is reaching by now its limits in miniaturisation. The key goal in molecular photonics is the development of photonic materials and devices based on organic (bio)molecules. The use of organic materials offers the advantage of easy fabrication, the possibility of synthesising and modifying organic compounds into the desired structures by molecular engineering and the tuning of a large variety of physical properties by small changes in the structure. Despite rapid progress in the field (see refs. [2–4] for the most recent reviews), demonstrations of functionality at the level of single molecules, for instance, switching, photon or charge transport, and energy conversion, are rather scarce.[5–8] Exciting enough, the advent of single-molecule techniques is offering nowadays the possibility of exploring the properties and assessing the functionality of molecular devices on an individual basis.

In recent years, single-molecule fluorescence spectroscopy (SMS) has consolidated as unique method to investigate the properties of individual emitters in complex systems at ambient conditions.[9–11] Fluctuations in the fluorescence–time trajectories of individual emitters contain detailed molecular-level statistical and dynamical information of the system. Quantum jumps between singlet and triplet states on individual molecules embedded in thin polymer films have been observed at room temperature.[12,13] Photon antibunching revealing the quantum character of single or coupled emitters,[14–17] on–off fluorescence blinking,[18] collective quantum jumps[18] and superradiance in strongly coupled systems[19–20] are only few examples of the quantum phenomena that can be readily observed at room temperature using single-molecule detection techniques. As such, the technique has reached its level of maturity to investigate and eventually manipulate photonic molecular systems with potential device functionality.

Yet, the road towards molecule-based optical devices is facing at least three clear challenges: 1) the actual development phase, where the physical properties to be tuned by synthetic methods have to match those that can be measured with current single-molecule techniques; 2) the testing and operation of individual devices using nanoscale instrumentation; and 3) the need to interface such nanometric-sized molecular

[a] *Dr. M. F. García-Parajó, G. S. Mosteiro, Dr. J. P. Hoogenboom, Dr. E. M. H. P. van Dijk, Prof. N. F. van Hulst*
Applied Optics Group, Faculty of Science & Technology
MESA+ Institute for Nanotechnology, University of Twente, P.O. Box 217
7500 AE Enschede (The Netherlands)
Fax: (+31) 53-489-3511
E-mail: m.f.garciaparajo@utwente.nl

[b] *Dr. J. Hernando*
Departament de Química, Universitat Autónoma de Barcelona UAB
Cerdanyola del Vallés (Spain)

 DOI: 10.1002/cphc.200400630

device to the macroscopic world. Herein, we discuss our efforts towards the design of molecular photonic wires and their investigation at the individual molecular level by optical means. The general idea of such a device is illustrated in Figure 1 a. Light is absorbed by one of the chromophores composing the

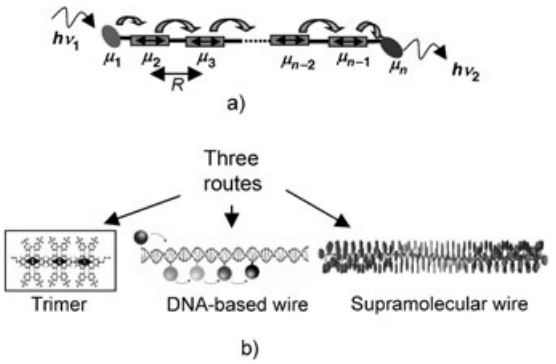

Figure 1. *a) Basic concept of a molecular-based photonic wire; b) three different approaches towards the design of molecular photonic wires.*

wire and "transmitted" towards a collecting chromophore from which a final photon is emitted. Three different synthetic approaches, as schematically shown in Figure 1 b, have been explored, namely: a) Perylene-based dimer and trimer assemblies; b) DNA-based unidirectional molecular wires; and c) One-dimensional multichromophoric polymers based on perylene polyisocyanides. Furthermore, we have applied SMS to investigate individual wires and demonstrate that both weak and strong dipole coupling interactions govern the properties of these well-ordered artificial systems. Finally, we discuss the performance of the wires in terms of their (bio)chemical stability and influence by the environment.

Energy-Transfer Mechanisms in Multichromophoric Systems

Multichromophoric systems can exhibit interesting optical and electronic properties due to the interactions between dye units that are near to each other. This may result in electron energy (exciton) transfer over the system, a process that constitutes the physical working mechanism in various kinds of relevant complex molecular aggregates, such as photosynthetic and autofluorescent proteins,[21,22] light-harvesting assemblies[23] and conjugated polymers.[24] Full understanding of the excitonic interaction between adjacent chromophores is therefore a necessary step when envisaging the design of molecular photonic wires.

In absence of orbital overlap, electron energy transfer between nearby chromophores is generally caused by the transition dipole moment coupling, an interaction whose strength (U) decreases with the third power of the intermolecular distance. The rate of the transfer process, however, is constrained by static (energy and geometry fluctuations) and dynamic (coupling to phonons) disorder in the system (Δ), which counterbalances the effect of dipole coupling on the optical properties of the assembly. Two limiting situations can be distinguished according to the U/Δ ratio.[25] For large U/Δ values (i.e., large coupling strength due to short interchromophoric distances, low disorder), coherent energy transfer between adjacent chromophores holds, whose individual electronic functions superimpose to yield new exciton states delocalised over the entire system, as indicated in Figure 2 a.[25] Accordingly, the as-

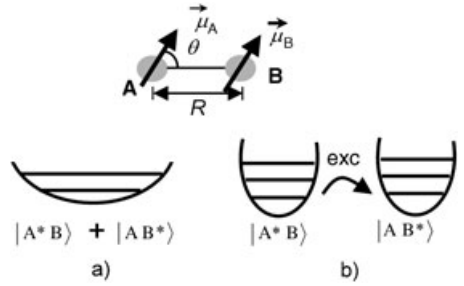

Figure 2. *Two limiting energy-transfer processes occurring on close-by molecules; a) In the strong coupling regime, the assembly behaves as a new single-quantum system, and the energy is delocalised over the entire system. b) In the weak coupling regime, the molecules behave as separate entities preserving their spectral properties. Incoherent energy transfer occurs from a donor to an acceptor molecule.*

sembly behaves as a new single-quantum system, whose optical properties significantly differ from those of the separate chromophores and critically depend on the orientation of the interacting dipoles. Whereas a head-to-tail alignment (J configuration) leads to an enhancement of the excited-state radiative rate (superradiance) together with red-shifted absorption and emission, a parallel transition dipole arrangement (H configuration) results in blue-shifted absorption followed by suppression of fluorescence emission.[25]

On the other extreme, very low U/Δ values (i.e., small coupling strength due to large interchromophoric distances, high disorder) lead to Förster-type incoherent energy transfer between nearby dyes (Figure 2 b), vibrational relaxation in the excited unit (donor) occurring before transfer to the adjacent chromophore (acceptor).[26] Consequently, the spectral properties of the interacting dyes are not altered. The efficiency of energy transfer is in this case given by $E_T=(1+(R/R_0)^6)^{-1}$, where R is the intermolecular separation and R_0 the distance at which the transfer efficiency equals 50%. R_0 is related to the spectral properties and relative orientation of the molecules by $R_0=0.211[\kappa^2 n^{-4} Q_D J(\nu)]^{1/6}$, where κ^2 is the orientation factor, Q_D is the quantum yield of the donor in the absence of the acceptor, n is the refractive index of the medium and $J(\nu)$ is the spectral overlap between donor emission and acceptor absorption spectra.

Both weak and strong coupling interactions on individual natural and artificial multichromophoric systems have been extensively studied in recent years.[15–17,19–24,27] On one side, SMS studies have focussed on complex systems containing a large number of chromophore units, such as light harvesting complexes[23] and multichromophoric conjugated polymers.[24] Furthermore, other natural multichromophoric systems containing a smaller number of chromophore units, such as the autofluorescent protein DsRed[22] and the allophycocyanin trimer from

Banana variabilis[21] have been investigated at the single-molecule level. Unfortunately the intrinsic complexity of those systems hampers full understanding of their collective behaviour. On the other side, some recent approaches have been devoted to the analysis of excitonic effects at the single-molecule level in simpler artificial multichromophoric systems intended to mimic the behaviour of natural systems. Energy transfer for a donor–acceptor pair has been investigated by using DNA as a rigid spacer and varying the interchromophoric distance,[28] and dendrimers have been employed to generate multichromophoric assemblies containing either one or two different types of chromophore units.[27] To attain optimal excitonic behaviour in multichromophoric assemblies, a well-defined close packing of the chromophores is thus required. Three different synthetic approaches towards the design of well-ordered one-dimensional multichromophoric arrays intended to work as molecular photonic wires are discussed below.

Perylene-Based Dimer and Trimer Photonic Wires

The simplest systems resembling molecular photonic wires are composed by two or three identical chromophores covalently linked in a parallel head-to-tail configuration. For that purpose, we have used tetra-*t*-butylphenoxy-perylene diimide as chromophore. Due to steric repulsion between the *t*-butylphenoxy branches in the perylene bay positions, the typical planar configuration of nonsubstituted perylenes is slightly distorted although the perylene main transition dipole moment still remains aligned along its long molecular axis, as illustrated in Figure 3.[20] Quantum mechanical calculations show that the resulting perylene-based dimers and trimers have a rigid structure with the individual units being perpendicular to each other, which prevents full extension of the π-conjugated path of the system. Under these conditions, and with interchromophoric distances of 1.3 nm, strong excitonic coupling is expected even at room temperature.

Figure 3 shows, as examples, fluorescent trajectories recorded at room temperature of an individual monomer (*a*), dimer (*c*) and trimer (*e*) perylene assembly. One single intensity level above the background is recovered on the perylene monomer (observed for 70% of the 110 molecules investigated) accompanied by the irreversible photobleaching of the molecule at $t = 20$ s. In contrast, two and three distinct intensity levels above the background are observed on the dimer and trimer assemblies, respectively. This situation is found for 70% of the dimers and 66% of the trimers investigated. The discrete intensity levels arise from the stepwise photodegradation of perylene units in the dimer and trimer and are a characteristic signature of multichromophoric systems.[21,22,24,27] The intensity ratios for the different levels in the dimer are (2:1) and (2.8:2.2:1) for the trimer system. The slight deviation observed for the trimer system with respect to the ideal intensity ratio (3:2:1) is ascribed to spectral changes upon photobleaching, while the emission quantum yield of the individual chromophores remains constant.[20] Indeed, bulk measurements show that the fluorescence quantum yield (Φ_f) of intact monomer, dimer and trimer molecules is very similar and close to one, but the absorption cross-section at $\lambda = 568$ nm does not scale with the number of chromophores.

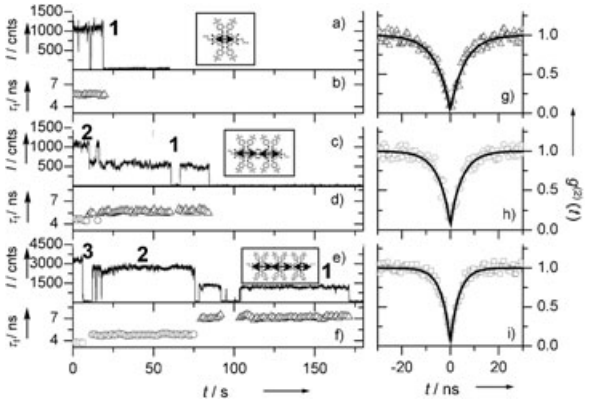

Figure 3. *a) and b) Fluorescence intensity trajectory (bin time = 50 ms) and excited lifetime τ_f for a monomer molecule. Each τ_f value derives from a monoexponential fitting to the photon arrival time decay built every 1.5 s. c) and d) Fluorescence intensity trajectory (bin time = 50 ms) and excited lifetime τ_f (bin time = 1.5 s) for a dimer molecule. (△) stand for τ_{f1} (lowest intensity level), while (○) stand for τ_{f2} (highest intensity level of the dimer). e) and f) Fluorescence intensity trajectory (bin time = 50 ms) and excited lifetime τ_f (bin time = 1.5 s) for a trimer molecule. (△) stand for τ_{f1} (lowest intensity level), (○) for τ_{f2} (intermediate level of the trimer) and (□) stand for τ_{f3} (highest intensity level of the trimer). g)–i) Experimental (symbols) and fitted (lines) second-order correlation function, $g^{(2)}(t)$ for a monomer molecule (g), highest level of a dimer molecule (h) and highest level of a trimer molecule (i). From the fitting: $g^{(2)}(0) = 0.04$ and $\tau_f = 6.1$ ns for the monomer (g); $g^{(2)}(0) = 0.08$ and $\tau_{f2} = 5.0$ ns for the highest level of the dimer (h); and $g^{(2)}(0) = 0.11$ and $\tau_{f3} = 3.7$ ns for the highest level of the trimer.*

To elucidate the occurrence of exciton coupling effects in the emission of perylene dimers and trimers, the time delay between consecutive emitted photons for individual molecules was measured.[14–17] Figures 3g–3i show the interphoton time distribution for a single perylene monomer (g) and the highest intensity levels of an individual dimer (h) and trimer (i), which follow the second-order correlation function $g^{(2)}(t)$ at short times. As expected, the perylene monomer exhibits a pronounced dip at $t = 0$ with $g^{(2)}(0) = 0.04$, which is consistent with its single-emitting character (antibunching behaviour). On the other hand, both the intact dimer and trimer display similar dips at $t = 0$, with $g^{(2)}(0) = 0.08$ for the dimer and $g^{(2)}(0) = 0.11$ for the trimer, in contrast with the values of $g^{(2)}(0) = 0.5$ and $g^{(2)}(0) = 0.67$ expected for two and three in-plane independent emitters, respectively. The low values of $g^{(2)}(0)$ obtained for both systems confirm their single-emitting character, consistent with the fact that, at a given moment in time, fluorescence arises from a single-emitting site. Such behaviour is a fingerprint for the occurrence of electron energy transfer in the assemblies, regardless of whether the separate dye units in the system are weakly[15,16] or strongly[20,29] coupled. Interestingly, the width of the dip in the $g^{(2)}(t)$ graphs in Figure 3 narrows with the number of interacting dye units. Since the dip width is related to the excited-state fluorescence lifetime, Figures 3g–3i hint to the occurrence of changes in the radiative rate with the number of interacting chromophores.

To further investigate this issue, the fluorescence lifetimes of monomer, dimer and trimer molecules were monitored in time, together with the fluorescence intensity, as shown in Figures 3 b, 3 d and 3 f. Simultaneously with intensity jumps in the dimer and trimer, fluorescence lifetime jumps are also observed. As shown in Figure 3 d, the dimer exhibits a lifetime of $\langle\tau_f\rangle = 4.6$ ns for the highest intensity level (two active units) and suddenly increases to $\langle\tau_f\rangle = 5.6$ ns on the lowest intensity level (one active unit), a value that is similar to that found for the perylene monomer ($\langle\tau_f\rangle = 5.6$ ns). Likewise, Figure 3 f shows sudden jumps in the excited fluorescence lifetime of the trimer. The recovered values are $\langle\tau_f\rangle = 3.8$, 4.8 and 7.1 ns for the highest (three active units), intermediate (two active units) and lowest (one active unit) intensity levels, respectively. The shorter fluorescence lifetimes obtained for both the intact dimer and the trimer are indicative of strong excitonic coupling interactions between the individual units composing the assemblies.[19,20,25] In fact, enhancement of the radiative rate (superradiance) and thus a shortening of the excited-state lifetime are expected for strongly interacting molecular systems arranged in a head-to-tail configuration (see above). Together with superradiance, we have also observed a smoothing out of the vibronic features in the spectrum of the dimeric and trimeric systems and a red-shifted emission spectrum, confirming coherent exciton delocalisation in the assemblies.[20,30]

The large majority of the molecules investigated showed excitonic interactions similar to those presented in Figure 3. The degree of superradiance, and thus the exciton delocalisation length, can be estimated according to the superradiance coherence factor L_s,[19] given by $L_s = k_{rad}(\text{level } n)/k_{rad}(\text{level } 1)$, where $k_{rad} = 1/\tau_f$ as $\Phi_f \approx 1$ in all cases, n corresponds to the highest and 1 to the lowest intensity levels of the assembly. For an ideal molecular assembly, where the excitation is completely delocalised, the L_s factors should be 2 for the dimeric and 2.9 for the trimeric systems, respectively.[19,20,25]

Figure 4 a shows the distribution per intensity level, of the excited-state lifetime obtained for 55 dimer molecules. As clearly observed, the lifetime distribution of the highest intensity level, that is, the intact dimer system, is shifted to shorter values of τ_f as compared to the distribution of the lowest intensity level, where only one chromophore is active. The average τ_f values are 4.8 ns when both units are active and $\langle\tau_f\rangle = 5.7$ ns with only one active unit. Figure 4 c shows the recovered $L_s = \tau_{f1}/\tau_{f2}$ distribution for the perylene dimers. The distribution varies from $L_s = 1$ to $L_s = 1.55$ with an average value of $L_s = 1.2 \pm 0.1$. As already mentioned, L_s is a measure of the exciton delocalisation length, and thus, the higher L_s, the stronger the coupling between the chromophores. A value of $L_s = 1$ indicates weak or no coupling at all. As observed in Figure 4 c, the large majority of the dimers show strong coupling interactions between their chromophores. Yet, the exciton delocalisation extent is considerably lower than that expected from an ideal system. This demonstrates that, in our case, disorder plays an important role in limiting the strength of coupling.[20,30] Thus, the local surrounding of the heterogeneous polymer host introduces energy variations from molecule to molecule, as well as changes in their photophysical properties. This is proven by the significant spread in fluorescence lifetimes and spectra measured for the perylene monomer (data not shown).

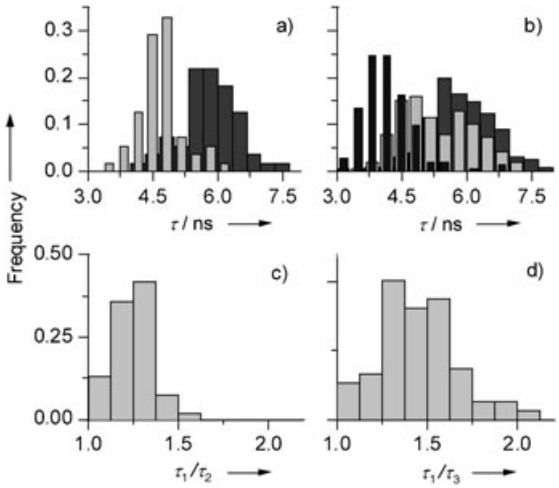

Figure 4. *a) Lifetime distributions for the different levels of 55 dimer molecules; b) Lifetime distributions for the different levels of 121 trimers investigated; c) Histogram of the τ_{f1}/τ_{f2} ratio for the dimers in (a); d) Histogram of the τ_{f1}/τ_{f3} ratio for the trimers in (b). $\langle\tau_{f2}\rangle = 4.8$ ns (light grey) and $\langle\tau_{f1}\rangle = 5.7$ ns (dark grey) for levels 2 (highest) and 1 (lowest) of the dimer molecules, respectively. $\langle\tau_{f3}\rangle = 4.1$ ns (black), $\langle\tau_{f2}\rangle = 5.3$ ns (light grey) and $\langle\tau_{f1}\rangle = 5.9$ ns (dark grey) for levels 3, 2 and 1, respectively, of the trimers investigated.*

A similar trend is also obtained when compiling the lifetime distributions for each intensity level on 121 perylene trimers. Figure 4 b shows a clear shift of the distributions to shorter values of τ_f with the number of interacting chromophores. Although strong excitonic coupling between the different units exist, the effect of static and dynamic disorder is also present, with an average superradiance coherence factor L_s of 1.5 ± 0.2, as shown in Figure 4 d, instead of 2.9 as expected for a fully delocalised trimer array.[20]

Both perylene-based dimer and trimer assemblies are examples of well-ordered multimolecular systems, where the excited-state energy is partially delocalised, and they constitute a first step towards the design of more complex systems. One could envisage, for instance, the inclusion of an antenna dye at a higher energy to capture and funnel the light toward the dimer or trimer "transmission" unit and the addition of a lower energy dye on the other extreme of the wire for final photon emission. In this way, efficient and rapid energy transfer from the antenna to the collector unit should, in principle, be achieved. Although possible, the design of such a molecular photonic wire by synthetic routes remains a challenge.

DNA-Based Molecular Photonic Wires

A more feasible route towards the design of molecular photonic wires is provided by the use of fluorescent dyes in combination with DNA as a rigid scaffold. The unique features of double-stranded DNA make it an ideally suited building block for nanoscaled molecular devices.[31] With a persistence length of 50 nm, DNA constitutes a stiff scaffold for the chromophores. In addition, DNA offers many well-developed labelling

strategies including hybridisation of labelled short complementary oligonucleotides and dye intercalation. Furthermore, the position and thus the distance between adjacent dyes can be controlled with sub-nanometric accuracy. Identical or different dyes can be easily incorporated at specific positions along the DNA strand, tuning in this way the directionality of the energy flow.[32,33]

Figure 5a shows a cartoon of the DNA-based photonic wire designed for our experiments. Five chromophores with considerable overlap between subsequent absorption and emission

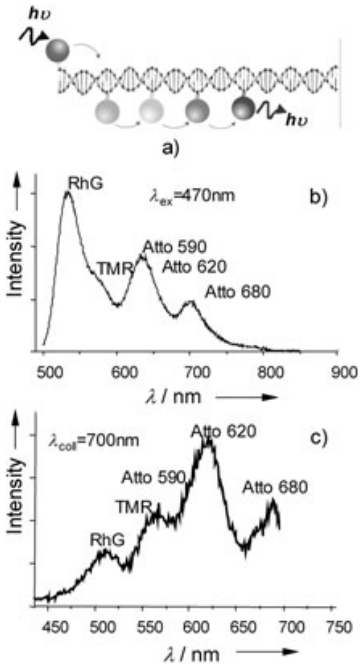

Figure 5. *a) DNA-based photonic wire containing five different chromophores. The distance between neighbouring dyes is 3.4 nm. b) Bulk emission spectrum of the DNA wires upon excitation of RhG at 470 nm. c) Bulk excitation spectrum recorded while collecting the emission at 700 nm.*

spectra (Rhodamine green (RhG), tetramethylrhodamine (TMR), Atto 590, Atto 620 and Atto 680) were covalently attached to single-stranded DNA fragments of various lengths (60 or 20 bases) using 6C linkers. Hybridisation of the labelled DNA fragments to the complementary DNA strand (60 base pairs) results in a construct containing five different chromophores positioned at well-defined distances. An interchromophoric distance of 10 base pairs, which corresponds to 3.4 nm, was chosen to maximise transfer efficiency between neighbouring dyes, while providing sufficient biochemical stability to the whole construct. Because of the distances involved and the random orientation between the dyes imposed by the linking strategy to DNA, weak excitonic interactions between adjacent units (FRET) are expected. The spatial extent of the wire is 13.6 nm, with an estimated overall energy-transfer efficiency of $\approx$70–80%, taking into account the spectral overlap between the different units and assuming random orientation of the chromophores ($\kappa^2 = 2/3$).

Figure 5b shows the bulk emission spectrum of the DNA wires as recorded in solution at a concentration of 10^{-7} M. The excitation wavelength used is 470 nm matching the absorption of RhG (first dye on the wire). In case of perfect FRET along the wire, one should essentially recover the emission spectrum of the last dye, that is, Atto 680. Instead, a complex emission spectrum is observed. Three main peaks are readily distinguished, which most probably correspond to the emission of RhG (left peak), a combination of the Atto 590 and Atto 620 emissions (middle peak) and, finally, emission of Atto 680 (right peak). The shoulder at $\lambda = 575$ nm corresponds to the emission of TMR. Since only RhG is efficiently excited at 470 nm (direct absorption from the other dyes at 470 nm is negligible), the observed emission must exclusively result from energy transfer between the chromophores composing the wire, which demonstrates the functionality of the construct. However, it is also clear that the extent of energy transfer to Atto 680 is far from perfect.

Since the measured bulk emission spectrum might result from a considerable number of partially non-hybridised DNA fragments, we also measured the excitation spectrum of the wires while collecting the fluorescence at $\lambda = 700$ nm, the maximum of emission of Atto 680. The excitation spectrum is shown in Figure 5c. Clearly, energy transfer between the different dyes occurs, including FRET from the first dye (RhG). From the emission/excitation spectra we estimate an overall FRET efficiency from RhG to Atto 680 of 20%, which is much lower than initially estimated. The lower extent of energy transfer might be due to incomplete hybridisation and/or unfavourable conformational orientation of the chromophores composing the wire.[7]

To gain more insight on the complex photophysical behaviour of the DNA-based photonic wires, we have performed SMS experiments by recording, simultaneously, the fluorescence intensity and emission spectra of a large number of individual wires upon excitation at $\lambda = 488$ nm. A typical fluorescence trajectory is shown in Figure 6a. The red trajectory corresponds to emission above 585 nm (i.e., emission from the last three dyes), while the green trajectory results from emission at $\lambda < 585$ nm. As clearly seen, a large number of intensity jumps occurs during recording of the fluorescence. Up to $t =$ 15 s, the fluorescence is dominated by emission of the last three dyes composing the wire—consistent with efficient FRET from RhG and probably a minor contribution from direct excitation of TMR. Equal contributions of the fluorescence in both channels occur between $t = 16.5$ and 17 s. Finally, from $t = 20$ s, and until photodissociation occurs ($t = 25$ s), the fluorescence is dominated by green emission, which indicates the loss of transfer (most probably due to photobleaching of one or more red-shifted units). Furthermore, during the observation time, the total fluorescence emission (green + red channels) is interrupted in several occasions ($t = 8$, 15 and 18 s) by the occurrence of long dark (nonemitting) periods. The simultaneous cessation of the fluorescence on the entire wire array is a clear signature of collective effects characteristic of coupled multichromophoric systems.[24,27]

The large intensity jumps are also correlated with spectral jumps. Figure 6b shows three different emission spectra of the same wire recorded at $t = 0$, 12 and 22 s. While at $t = 0$ s the

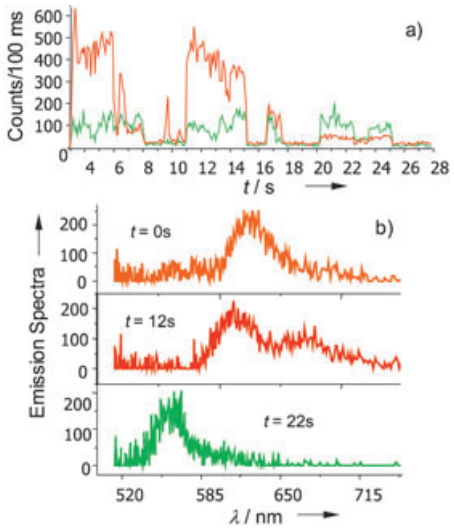

Figure 6. *a) Fluorescence trajectory of an individual DNA photonic wire with a bin time of 100 ms. b) Series of emission spectra recorded at* t = *0, 12 and 22 s. The fluorescence signal was separated from the excitation light using a long-pass filter at 500 nm and split into two equally intense signals using a nonpolarising beam splitter. One of the branches was sent directly to a CCD camera (Andor, DV437-BV) for spectral recording. Fluorescence spectra were collected with an integration time of 1 s. The second half of the fluorescence signal was further split in two distinct spectral windows using a dichroic mirror centred at 585 nm and sent to two separate APD detectors.*

spectrum is dominated by emission of the fourth dye, at $t = 12$ s emission from a combination of third, forth and fifth dye is observed. At $t = 22$ s only emission from RhG (first dye) is observed. This intricate behaviour results from differences in FRET efficiencies along the wire, which are most probably caused by orientational changes, spectral fluctuations between absorption and emission spectrum of adjacent dyes and/or electron transfer favoured by the presence of the DNA scaffold. Current experiments at the single-molecule level should shed light on the underlying reasons for the reduction of the overall photon-transfer efficiency of these systems.

We have observed that approximately 10% of the wires exhibit overall FRET efficiencies up to 90%.[7] This represents an unprecedented unidirectional photon transfer at room temperature over a distance of 13.6 nm, with a spectral range of 200 nm.[7] On the other hand, the rigidity and biochemical stability of such a complex system has to be seriously investigated before taking full advantage of DNA as building block for the design of well-ordered molecular wires.

One-Dimensional Multichromophoric Polymers Based on Perylene Polyisocyanides

One way of obtaining a rigid scaffold for the ordered attachment of chromophores is by using helical polyisocyanides.[34] These supramolecular systems are obtained by polymerisation of isocyanide monomers. Due to their particular helical nature, the side groups are all placed at exact distances and precise positions with respect to each other. By using amide functions in the side groups, hydrogen-bonding arrays are formed along the polymer backbone rigidifying even further the polymer and stabilising the helical structure.[34] Furthermore, polymers with a length of hundreds of nanometres can be readily synthesised. We have used diimides of perylene-3,4,9,10-tetracarboxilic acid as chromophores to create long arrays of the photonic polymer.[8,35]

Figure 7a shows the structure of the perylene polyisocyanide together with a schematic 3D drawing of the polymer (Figure 7b). The perylene dyes are attached to the polymer backbone in four parallel stacks. The adjacent dye molecules in one stack are found to be 0.42 nm apart with a twist angle of 22°.[36] For such a chromophoric ordering, strong excitonic interactions between the chromophores and over the entire

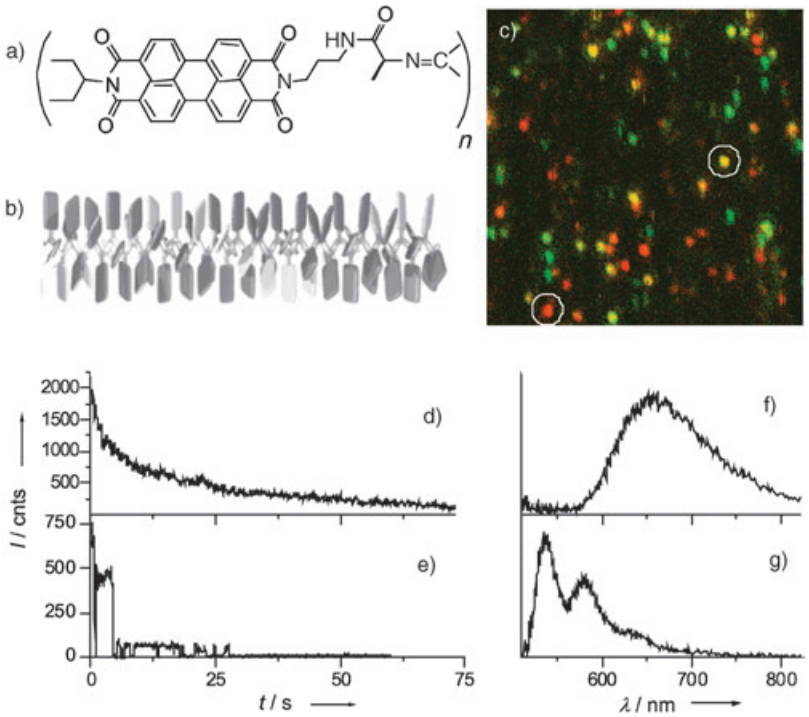

Figure 7. *a) Structure of the perylene polyisocyanide; b) 3D drawing of a single polymer fibre; c) Confocal scan of individual perylene polyisocyanides embedded in a thin PMMA layer (256×256 pixels; 1 kHz scan rate). A polarising beam splitter was used on the detection side and the two resultant signals sent to two APD detectors providing polarisation-sensitive single-molecule detection. Two spots are encircled in the figure, that is, a yellow spot whose total intensity and spectral features are shown in (d) and (f); and a red spot whose total fluorescence and spectral properties are shown in (e) and (g).*

polymer are expected. Bulk absorption and emission spectra show that, indeed, interactions between the perylene molecules in the polymer already occur in the ground state, pointing to the existence of excitonic effects.[8] Furthermore, the bulk fluorescence spectrum of the perylene polymer is markedly different from that of the monomer, with a considerably red-shifted emission that is independent from the sample concentration and a much longer fluorescence lifetime ($\tau_f = 19.6$ ns for the polymer vs. $\tau_f = 3.9$ ns for the monomer).[8,35] These features indicate that emission mainly arises from intramolecular excimerlike species in the polymer, resulting from the short distances and the stacked arrangement of the perylene molecules.[37]

To investigate in more detail the nature of the fluorescence emission in the perylene polymers at the individual level, we prepared spin-coated diluted solutions of the polymers (10^{-8} M in PMMA) on glass substrates. A typical single-molecule confocal image is shown in Figure 7c, where fluorescent spots with distinct colour and brightness are visible. The presence of well-defined polarised emission (colour of some spots being either green or red) is indicative for unique dipole emission and thus single-molecule emission. On the other hand, the yellow colour of some fluorescent spots is due to unpolarised or randomly polarised emission, which results from adding multiple molecules with random in-plane orientation (combination of red and green) in one spot. In addition to the polarisation of the emission, also the fluorescence intensity and emission spectra of individual spots were investigated.

Two clearly different behaviours could be distinguished upon recording of individual fluorescent trajectories and emission spectra. The emitters yielding unpolarised emission (yellow spot encircled in Figure 7c) showed a monotonous decrease of the fluorescence intensity in time, as shown in Figure 7d, together with a broad red-emission spectrum (Figure 7f). These results suggest that the intensity originates from a large number of fluorescent sites, whose successive photobleaching leads to a continuous decrease of the emission. The red-shifted spectrum is consistent with an excimerlike emission, as already observed on bulk experiments. The other type of emitter displaying a defined polarisation emission behaved completely different. A typical fluorescence trajectory is shown in Figure 7e, together with its emission spectrum (Figure 7g) corresponding to the red-marked spot in Figure 7c. The trajectory exhibits sudden jumps in the intensity, which indicate that only a discrete number of emissive sites are present. The different jumps arise from discrete photobleaching of perylene molecules. Interestingly, the emission spectrum shown in Figure 7g resembles that of the perylene monomer. Similarly, simultaneous quantum jumps of the intensity to the background level are also observed, which suggests that energy transfer is taking place between the perylene units and is consistent with the collective behaviour characteristic of multichromophoric systems.[24,27] The absence of such collective non-fluorescent states on the emitting species displaying the continuous decay suggest that these species emit independently.

The observed different emission behaviour occurring in one sample suggests that two different perylene "species" may be present in the polymer mixture, that is, perylene species that are dangling around, most likely in the ill-defined polymer end groups or in the form of short oligomers, and perylene species that are well-organised, probably located in the main part of the polymer. The stepwise behaviour of the green- and/or red-coloured spots in the confocal image is reminiscent of the behaviour obtained in multichromophoric systems.[27] In our particular case, the polyisocyanide will force several perylene species together in a confined space and in a less ordered arrangement. This will be the case for the more flexible polymer end groups or short oligomers where the helical structure is not fully accomplished, as depicted in Figure 8a. In fact, studies on polyisocyanides have proven that at least 10–15 repeat units are necessary to obtain a stable helical structure. As in other multichromophoric systems, after excitation the energy is transferred to the perylene with the lowest-lying energy state from which emission will proceed hence explaining the polarised emission together with the monomerlike spectrum.

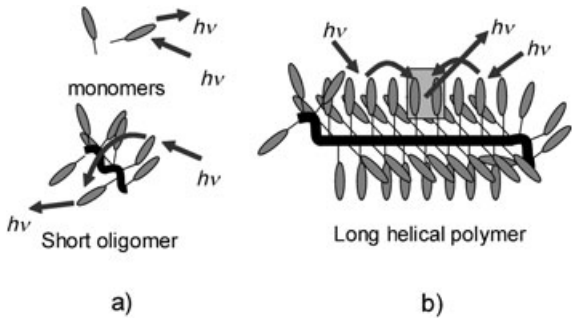

Figure 8. *Cartoon illustrating the two kinds of species found in the experiments: a) Monomer and/or short oligomers and b) long helical polymers. In (a) energy transfer occurs between close-by chromophores, while in (b) excimers act as sinks for the exciton, reducing the extent of delocalisation of the electronic excitation.*

On the other hand, the excimer emission stems from the well-defined central part of the polyisocyanides in which the perylene species are all located on top of each other in exactly the same geometry. The observed continuous fluorescence decay of the single polymer fibres is consistent with the formation, upon photoexcitation, of many excimer sites along the polymer chain—all with different directions—resulting in the randomly polarised fluorescence and the broad excimerlike emission spectrum. After photoexcitation, strong excitonic coupling between the highly organised perylene side chains of the polymer is expected to occur. However, due to the well-defined and close-by organisation, the excitons are quenched via the formation of excimer species between two or more perylene groups, as illustrated in Figure 8b. As such, excimers will act as sinks for the exciton, limiting the extent of the delocalisation of the electronic excitation and leading to the observed fluorescence emission.

The question whether the two types of behaviour are displayed by a single polymer molecule, or separately by short oligomers in a random coil conformation and by rigid rod polymers, is a difficult one to solve based on single-molecule

fluorescence data solely. Instead, a combination of atomic force and confocal microscopy can provide correlated information on the physical size of both "species" and their photophysical behaviour. We have performed such type of simultaneous experiments and have been able to prove that the multichromophoric behaviour arises from short oligomers or even perylene monomers, while the excimerlike emission indeed proceeds from the long well-ordered polymer isocyanides.[8]

Our results thus demonstrate the successful design of long polyisocyanide polymers with pendant perylene dyes. The persistent length of these supramolecular structures is 76 nm, being stable to at least 90 °C.[35] Furthermore, individual fibres of several hundred nanometres could be synthesised incorporating several thousand perylenes.[35] The photophysical properties of the individual arrays are unfortunately dominated by excimer formation, which reduces the extent of the exciton delocalisation, thus hampering the performance of the polymers as truly photonic molecular wires. Current synthesis efforts are focussed on the design of similar polymer-based polyisocyanide arrays incorporating other type of chromophore less prone to π stacking and, alternatively, exploiting the desirable advantages of perylene as highly efficient dyes, by extending the conjugation length between the dye and the isocyanide, in an effort to increase the interchromophoric distances and minimise the chances of excimer formation.

Conclusions

Three different approaches towards the design of one-dimensional multimolecular arrays intended to work as molecular photonic wires have been discussed in this Minireview. While perylene-based dimer and trimer arrays showed coherent exciton delocalisation at room temperature, DNA-based unidirectional molecular wires exhibited incoherent energy transfer between neighbouring dyes. Finally, one-dimensional multichromophoric polymers based on perylene polyisocyanides show emission arising from multiple excimer sites formed along the long polymer wire.

The performance of the photonic wires shown in this study is greatly influenced by the well-defined ordering of the chromophores, and the (bio)chemical stability of the assemblies. One could envisage the design of more complex structures combining strong and weak coupling interactions between the different units composing the wire in order to achieve optimum photon transfer. For instance, antenna complexes, in the form of one or more dyes absorbing at high energy, could be inserted at one end of the wire. FRET between the antenna and a transmission unit, composed by strong coupled chromophores, should then serve for rapid and efficient transfer of energy to a collecting dye from which light is finally emitted. Perylene-based multichromophoric arrays, such as the trimers or the polyisocyanide polymers shown herein, would, in principle, be ideal candidates to work as transmission units. In the latter case, π stacking could be prevented by increasing the separation between the perylene units composing the polymer. In combination with single-molecule techniques and scanning probe methods, these new synthetic approaches should lead in the near future to efficient and reliable photonic wires with true device functionality.

Acknowledgements

The authors thank J. J. Garcia-Lopez, M. Crego-Calama and D. Reinhoudt for synthesising the perylene dimers and trimers; P. de Witte, A. Rowan and R. Nolte for the synthesis of the perylene polyisocyanide polymers. We also thank M. Heilemann, P. Tinnefeld and M. Sauer for fruitful discussions and sharing of data concerning the DNA-based molecular wires. J. Korterik and F. Segerink are gratefully acknowledged for technical support. J.H. thanks the EC program IHP-99 for a Marie Curie Fellowship (HPMF-CT 2002–01698). G.S.M and E.M.H.P.v.D. acknowledge support from the Dutch Foundation of Fundamental Research of Matter (FOM). J.P.H. thanks the Volkswagen Foundation (VW), research priority area in "Single Molecules", for financial support.

Keywords: energy transfer · FRET (fluorescence resonance energy transfer) · molecular devices · photonics · single-molecule studies

[1] See for instance news feature *"Wired for success"* in D. Appell, *Nature* **2002**, *419*, 553.
[2] B. L. Feringa, R. A. van Delden, N. Koumura, E. M. Geertsema, *Chem. Rev.* **2000**, *100*, 1789.
[3] B. L. Feringa, *Acc. Chem. Res.* **2001**, *34*, 504.
[4] M. Grätzel, *Nature* **2001**, *414*, 338.
[5] T. Hugel, N. Holland, A. Cattani, L. Moroder, M. Seitz, H. E. Gaub, *Science* **2002**, *296*, 1103.
[6] M. Irie, T. Fukaminato, T. Saski, N, Tamai, T. Kawai, *Nature* **2002**, *420*, 759.
[7] M. Heilemann, P. Tinnefeld, G. Sanchez Mosteiro, M. F. Garcia-Parajo, N. F. van Hulst, M. Sauer, *J. Am. Chem. Soc.* **2004**, *126*, 6514.
[8] J. Hernando, P. A. J. de Witte, E. M. H. P. van Dijk, J. Korterik, R. J. M. Nolte, A. E. Rowan, M. F. Garcia-Parajo, N. F. van Hulst, *Angew. Chem.* **2004**, *116*, 4137; *Angew. Chem. Int. Ed.* **2004**, *43*, 4045.
[9] X. S. Xie, J. K. Trautman, *Annu. Rev. Phys. Chem.* **1998**, *49*, 441.
[10] Special issue in *Science* **1999**, *283*, 1670.
[11] *Single Molecule Spectroscopy, Chemical Physics* (Eds.: R. Rigler, M. Orrit, T. Basché), Springer, Heidelberg, **2002**, 67.
[12] T. Ha, Th. Enderle, D. Chemla, P. R. Selvin, S. Weiss, *Chem. Phys. Lett.* **1997**, *271*, 1.
[13] J. A. Veerman, M. F. Garcia-Parajo, L. Kuipers, N. F. van Hulst, *Phys. Rev. Lett.* **1999**, *83*, 2155.
[14] T. Basché, W. E. Moerner, M. Orrit, H. Talon, *Phys. Rev. Lett.* **1992**, *69*, 1516; L. Fleury, J.-M. Segura, G. Zumofen, B. Hecht, U. P. Wild, *Phys. Rev. Lett.* **2000**, *84*, 1148; B. Lounis, W. E. Moerner, *Nature* **2000**, *407*, 491.
[15] P. Tinnefeld, K. D. Weston, T. Vosch, M. Cotlet, T. Weil, J. Hofkens, K. Müllen, F. C. De Schryver, M. Sauer, *J. Am. Chem. Soc.* **2002**, *124*, 14310.
[16] G. Sánchez-Mosteiro, M. Koopman, E. M. H. P. van Dijk, J. Hernando, N. F. van Hulst, M. F. García-Parajó, *ChemPhysChem* **2004**, *5*, 1782.
[17] C. G. Hübner, G. Zumofen, A. Renn, A. Herrmann, K. Müllen, T. Basché, *Phys. Rev. Lett.* **2003**, *91*, 093903.
[18] R. M. Dickson, A. B. Cubitt, R. Y. Tsien, W. E. Moerner, *Nature* **1997**, *388*, 355; M. F. García-Parajo , G. M. J. Segers-Nolten, J.-A. Veerman, J. Greve, N. F. van Hulst, *Proc. Natl. Acad. Sci. USA* **2000**, *97*, 7237; J. Hofkens, W. Schroeyers, D. Loos, M. Cotlet, F. Köhn, et al. , *Spectrochim. Acta Part A* **2001**, *57*, 2003; T. Vosch, J. Hofkens, M. Cotlet, F. Köhn, H. Fujiwara, R. Gronheid, K. Van der Biest, T. Weil, A. Herrmann, K. Müllen, S. Mukamel, M. Van der Auweraer, F. C. De Schryver, *Angew. Chem.* **2001**, *113*, 4779; *Angew. Chem. Int. Ed.* **2001**, *40*, 4643; J. Hernando, M. van der Schaaf, E. M. H. P. van Dijk, M. Sauer, M. F. Garcia-Parajo, N. F. van Hulst, *J. Phys. Chem. A.* **2003**, *107*, 43.

[19] M. Lippitz, C. G. Hübner, T. Christ, H. Eichner, P. Bordat, A. Herrmann, K. Müllen, T. Basche, *Phys. Rev. Lett.* **2004**, *92*, 103001.
[20] J. Hernando, J. P. Hoogenboom, E. M. H. P. van Dijk, J. J. García-Lopez, M. Crego-Calama, D. N. Reinhoudt, N. F. van Hulst, M. F. García-Parajó, *Phys. Rev. Lett.* **2004**, *93*, 236404.
[21] L. Ying, X. S. Xie, *J. Phys. Chem. B* **1998**, *102*, 10399.
[22] M. F. Garcia-Parajo, M. Koopman, E. M. H. P. van Dijk, V. Subramaniam, N. F. van Hulst, *Proc. Natl. Acad. Sci. USA* **2001**, *98*, 14392.
[23] M. Wu, P. M. Goodwin, W. P. Ambrose, R. A. Keller, *J. Phys. Chem.* **1996**, *100*, 17406; M. A. Bopp, Y. Jia, L. Li, R. J. Cogdell, R. M. Hochstrasser, *Proc. Natl. Acad. Sci. USA* **1997**, *94*, 10630; A. M. van Oijen, M. Ketelaars, J. Köhler, T. J. Aartsma, J. Schmidt, *Science* **1999**, *285*, 400.
[24] D. A. Bout, W. Yip, D. Hu, D. Fu, T. M. Swager, P. F. Barbara, *Science* **1977**, *277*, 1074; D. Hu, J. Yu, P. F. Barbara, *J. Am. Chem. Soc.* **1999**, *121*, 6936; T. Huser, M. Yan, L. J. Rotherberg, *Proc. Natl. Acad. Sci. USA* **2000**, *97*, 11187; J. G. Müller, U. Lemmer, D. Raschke, A. Anni, U. Scherf, J. M. Lupton, J. Feldmann, *Phys. Rev. Lett.* **2003**, *91*, 267403.
[25] M. Kasha, H. R. Rawls, M. Ashaf El-Bayoumi, *Pure Appl. Chem.* **1965**, *11*, 371; A. S. Davydov, *Theory of Molecular Exciton*, McGraw-Hill, New York, **1962**.
[26] T. Förster in *Modern Quantum Chemistry* (Ed.: O. Sinanoglu), Academic Press, New York, **1965**.
[27] J. Hofkens, M. Maus, T. Gensch, T. Vosch, M. Cotlet, F. Köhn, A. Herrmann, K. Müllen, F. C. de Schryver, *J. Am. Chem. Soc.* **2000**, *122*, 9278; M. Cotlet, R. Gronheid, S. Habuchi, A. Stefan, A. Barbafina, K. Müllen, J. Hofkens, F. C. De Schryver , *J. Am. Chem. Soc.* **2003**, *125*, 13609.
[28] A. A. Deniz, M. Dahan, J. R. Grunwell, T. Ha, A. E. Faulhaber, D. S. Chemla, S. Weiss, P. G. Schultz, *Proc. Natl. Acad. Sci. USA* **1999**, *96*, 3670.
[29] C. Hettich, C. Schmidt, J. Zitzmann, S. Kühn, I. Gerhard, V. Sandoghdar, *Science* **2002**, *298*, 385.
[30] J. Hernando, E. M. H. P. van Dijk, J. Hoogenboom, M. F. Garcia-Parajo, N. F. van Hulst, unpublished results.
[31] See for instance Physics World, November **2004**, feature *"Molecular devices and machines"*, http://physicsweb.org/articles/world/17/11.
[32] S. Vyawahare, S. Eyal, K. D. Mathews, S. Quake, *Nano Lett.* **2004**, *4*, 1035.
[33] P. Tinnefeld, M. Heilemann, M. Sauer, *ChemPhysChem* **2005**, *6*, 217.
[34] J. J. L. M. Cornelissen, J. J. J. M. Donners, R. de Gelder, W. S. Graswinckel, G. A. Metselaar, A. E. Rowan, N. A. J. M. Sommerdijk, R. J. M. Nolte, *Science* **2001**, *293*, 676.
[35] J. Hernando, P. A. J. de Witte, E. M. H. P van Dijk, J. Korterik, R. J. M. Nolte, A. E. Rowan, N. F. van Hulst, M. F. García-Parajó, unpublished results.
[36] P. A. J. deWitte, M. Castriciano, J. J. L. M. Cornelissen, L. MonsQ-Scolaro, R. J. M. Nolte, A. E. Rowan, *Chem. Eur. J.* **2003**, *9*, 1775.
[37] W. E. Ford, P. V. Kamat, *J. Phys. Chem.* **1987**, *91*, 6373; P. B. Bisht, K. Fukuda, S. Hirayama, *Chem. Phys. Lett.* **1996**, *258*, 71; S. Akimoto, A. Ohmori, I. Yamazaki, *J. Phys. Chem. B* **1997**, *101*, 3753, and references therein.

Received: December 17, 2004
Revised: March 7, 2005

